

The nature of magnetic excitations in the high-field phase of α -RuCl₃

A. N. Ponomaryov,^{1,*} L. Zviagina,¹ J. Wosnitzer,^{1,2} P. Lampen-Kelley,^{3,4} A. Banerjee,^{5,†} J.-Q. Yan,³ C. A. Bridges,⁶ D. G. Mandrus,^{4,7} S. E. Nagler,⁵ and S. A. Zvyagin^{1,‡}

¹*Dresden High Magnetic Field Laboratory (HLD-EMFL) and Würzburg-Dresden Cluster of Excellence ct.qmat, Helmholtz-Zentrum Dresden-Rossendorf, 01328 Dresden, Germany*

²*Institut für Festkörper- und Materialphysik, TU Dresden, 01062 Dresden, Germany*

³*Materials Science and Technology Division, Oak Ridge National Laboratory, Oak Ridge, TN 37821, U.S.A.*

⁴*Department of Materials Science and Engineering, University of Tennessee, Knoxville, TN 37821, U.S.A.*

⁵*Neutron Scattering Division, Oak Ridge National Laboratory, Oak Ridge, TN 37831, U.S.A.*

⁶*Chemical Science Division, Oak Ridge National Laboratory, Oak Ridge, TN 37821, U.S.A.*

⁷*Materials Science and Technology Division, Oak Ridge National Laboratory, Oak Ridge, TN 37821, USA*

(Dated: June 25, 2020)

We present comprehensive electron spin resonance (ESR) studies of in-plane oriented single crystals of α -RuCl₃, a quasi-two-dimensional material with honeycomb structure, focusing on its high-field spin dynamics. The measurements are performed in magnetic fields up to 16 T, applied along the [110] and [100] directions. Several ESR modes are detected. Combining our findings with recent inelastic neutron- and Raman-scattering data, we identify most of the observed excitations. Most importantly, we show that the low-temperature ESR response beyond the boundary of the magnetically ordered region is dominated by single- and two-particle processes with magnons as elementary excitations. Peculiarities of the excitation spectrum in the vicinity of the critical field are discussed.

Spin systems with honeycomb structures have recently attracted a great deal of attention, in particular in connection with the Kitaev–Heisenberg model [1]. The model predicts a variety of magnetic phases, ranging from the conventional Néel state to a quantum spin liquid, with the excitation spectrum formed by spin-flip excitations, fractionalized into gapped flux excitations and gapless Majorana fermions [2]. α -RuCl₃ has been proposed as one of the prime candidates to test this model [3]. In this material, the multiorbital $5d t_{2g}$ state can be mapped into a single orbital state with effective pseudospins $j_{eff} = 1/2$. The spins are arranged into a two-dimensional (2D) honeycomb lattice [Fig. 1(a)] with bond-dependent interactions, defined by the Kitaev parameter K in the Hamiltonian:

$$\mathcal{H} = \sum_{\langle ij \rangle} \left[J \mathbf{S}_i \cdot \mathbf{S}_j + K S_i^\gamma S_j^\gamma + \Gamma \left(S_i^\alpha S_j^\beta + S_i^\beta S_j^\alpha \right) \right] - \mu_B \sum_i \mathbf{B} \cdot \mathbf{g} \cdot \mathbf{S}_i. \quad (1)$$

Here, S_i and S_j are spin-1/2 operators at site i and j , respectively, J is the Heisenberg exchange parameter, Γ represents a symmetric off-diagonal term, μ_B , \mathbf{B} , and \mathbf{g} correspond to the Bohr magneton, magnetic field, and g tensor, respectively (α and β are perpendicular to the Kitaev spin axis γ). A number of sets of parameters of the generalized Kitaev–Heisenberg model for α -RuCl₃ have been proposed (for review see, e.g., [4]). Below $T_N \sim 7$ K, the system undergoes the transition into 3D long-range zigzag magnetic ordered phase [5], associated with a triple-layer structure modulation in the direction

perpendicular to the honeycomb direction [phase AF1 in Fig. 1(b)]. Magnetic ordering is suppressed under the application of magnetic field B_c [6], followed by a partial polarization of the ground state [7]. In addition, a signature of the second phase (AF2) has been detected between B_c^* and B_c [8–10]. For $H \parallel [110]$, the critical fields are $B_c^* = 6.1$ and $B_c = 7.3$ T, and these converge at $B_c = 7.6$ T as one moves towards $H \parallel [100]$, where the separation is small, if not zero [9].

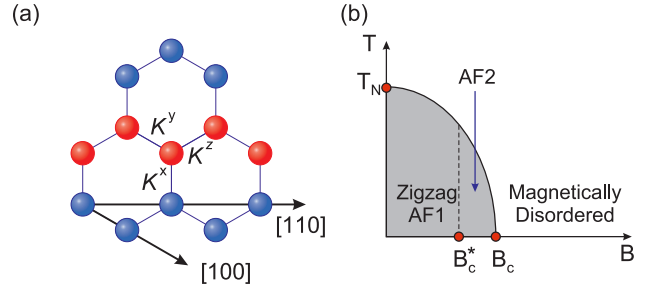


FIG. 1. (a) Schematic view of the honeycomb structure, showing the [100] and [110] axes relative to the Ru–Ru bonds. Ru ions from adjacent zigzag chains are shown by different colors. (b) Schematic temperature–field phase diagram for α -RuCl₃. AF1 and AF2 correspond to different low-temperature antiferromagnetically ordered phases.

One striking peculiarity of the spin dynamics in α -RuCl₃ is the presence of a broad excitation continuum, which has been interpreted as a potential signature of fractionalized Majorana excitations [11–14]. It can be observed up to well above 100 K, indicating the rather high energy scale of magnetic interactions in this compound. The continuum remains present well below T_N , when the ground state is magnetically ordered and the low-energy

excitation spectrum is formed by two antiferromagnetic-resonance (AFMR) modes [15–17]. Based on that, α - RuCl_3 was proposed to be in close proximity to the predicted Kitaev quantum spin liquid [12]. In the field-induced disordered phase the continuum is also present and gapped, with the gap gradually increasing with the applied magnetic field [8, 18–21].

Alternatively, the continuum can be described in terms of incoherent multimagnon processes [22, 23]. In line with that, recent calculations [4] points toward the physics of the strongly interacting and mutually decaying magnons, not to that of the fractionalized excitations.

Recent high magnetic field spectroscopy measurements revealed a very rich excitation spectrum in the field-induced magnetically disordered phase [15, 18–21], including several modes below the continuum. The remarkably large slope of some of them implies the presence of transitions with $\Delta S = 2$ (contrary to $\Delta S = 1$, expected for conventional one-particle excitations in $S = 1/2$ systems) [15]. This observation strongly suggested that the high-field spin dynamics in α - RuCl_3 has an emergent multiparticle nature, rising important question on the nature of the observed excitations.

To understand the complex spin dynamics in α - RuCl_3 , a comparative analysis of available experimental data is essential. Unfortunately, one critical shortcoming of the majority of magnetic studies of α - RuCl_3 comes from ignoring its in-plane anisotropy, which makes such a comparison challenging or even impossible. The anisotropy appears to be rather pronounced, as followed from high-field electron spin resonance [15] and magnetic susceptibility [9, 24] measurements, suggesting the presence of the Kitaev parameter K and symmetric off-diagonal spin exchange Γ (Eq. 1) as two key sources of the anisotropy [24, 25].

ESR is traditionally recognized as one of the most sensitive high-resolution spectroscopy tools for studying the spin dynamics in strongly correlated electron systems, capable to probe not only conventional magnons, but also fractional excitations (such as spinons and solitons [26–29]), the property of magnetic materials with quantum spin liquid ground states. Here, we present results of high-field tunable-frequency ESR studies of α - RuCl_3 , focusing on its spin dynamics in the field-induced magnetically disordered phase.

The measurements were performed on high-quality single crystals from the same batch as reported previously [15]. The plate-like samples were prepared using a vapor-transport technique starting from pure RuCl_3 powder and have typical sizes of $3 \times 3 \times 0.5 \text{ mm}^3$. The experiments were performed employing a 16 T transmission-type multifrequency ESR spectrometer, similar to that described in Ref. [31]. A set of backward-wave oscillators, Gunn diodes, and VDI microwave sources (Virginia Diodes Inc, USA) was used, allowing us to study magnetic excitations in a broad quasi-continuously covered frequency range,

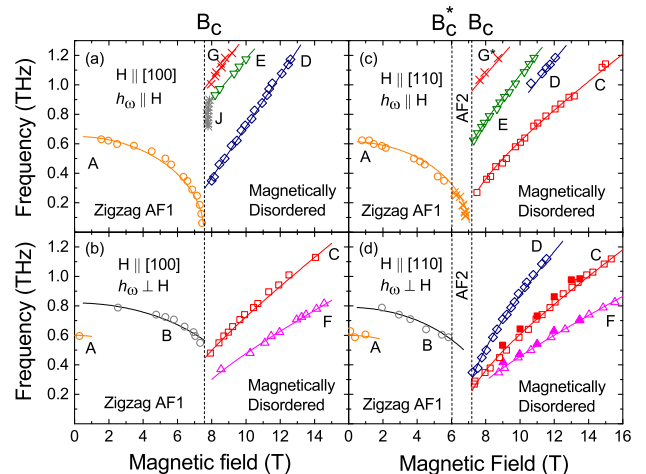


FIG. 2. Frequency-field dependences of magnetic excitations in α - RuCl_3 for $H \parallel [100]$ (a, b) and $H \parallel [110]$ (c, d) ($h_\omega \parallel H$ (a, c), $h_\omega \perp H$ (b, d), where h_ω is the magnetic component of the THz radiation; $T = 1.5 \text{ K}$). Absorptions denoted by crosses were observed using unpolarized radiation. Solid lines are guides to the eye. The vertical dashed lines indicate critical fields as determined in Ref. [9]. The closed squares and triangles in (d) denote inelastic neutron scattering data from Ref. [10].

from 0.05 to 1.2 THz (corresponding to an energy range of about 0.2 - 5 meV). The experiments were performed in the Voigt configuration with magnetic fields $H \parallel [100]$ and $H \parallel [110]$ [i.e., applied parallel and perpendicular to a Ru-Ru bond direction, respectively, Fig. 1(a)]. Fine orientation of the samples was done *in situ*, employing a goniometer with the rotation axis normal to honeycomb layers. A wire-grid polarizer was installed just before the sample, allowing us to select the polarization of the incident THz radiation with respect to the applied magnetic field and crystallographic axes.

The frequency-field dependences of polarized-ESR in α - RuCl_3 for $H \parallel [100]$ and $H \parallel [110]$ are shown in Fig. 2. Some examples of polarized-ESR measurement data are shown in Supplemental Material [30]. Two modes were observed in the low-field zigzag ordered phase, as reported previously [15]. These excitations (modes A and B) correspond to conventional relativistic AFMR modes, excited at the Γ point, with the zero-field frequencies 0.62 and 0.8 THz [17]. Both modes exhibit pronounced softening in magnetic field. The low-frequency AFMR mode A is dominantly excited when $h_\omega \parallel H$, while the mode B corresponds to excitations with $h_\omega \perp H$. At low fields, mode A was observed also when $h_\omega \perp H$. Such an unusual behavior can be explained by a change in domain populations, as suggested by neutron-scattering studies [8]. Detailed spin-wave-theory analysis of the AFMR spectrum (including the polarization dependence

of magnetic excitations) was performed by Wu et al. [17], revealing an overall good agreement with the obtained experimental data.

For both orientations of applied magnetic field, the intensity of the AFMR modes decreases significantly when approaching the critical region. These changes can be particularly well seen in unpolarized-ESR spectra [Figs. 3 and 4]. Remarkably, our ESR measurements revealed the presence of AFMR mode A not only below B_c^* , but also between B_c^* and B_c [Fig. 2(c)]. It has been recently proposed, that the antiferromagnetic interlayer coupling in α -RuCl₃ results in a triple-layer structure modulation in the direction perpendicular to the honeycomb direction (corresponding to the magnetic order 3f-zz), while the ferromagnetic interaction would lead to zigzag ordered state with a unit cell of six layers (6f-zz); the latter is likely realized in α -RuCl₃ between B_c^* and B_c [32]. Based on this assumption, the observation of the mode A in the AF2 phase suggests the co-existence of the 3f-zz and 6f-zz magnetic structures in this narrow intermediate field range [Fig. 1(b)]. More details of high-field magnetic-structure studies of α -RuCl₃ will be reported elsewhere [33].

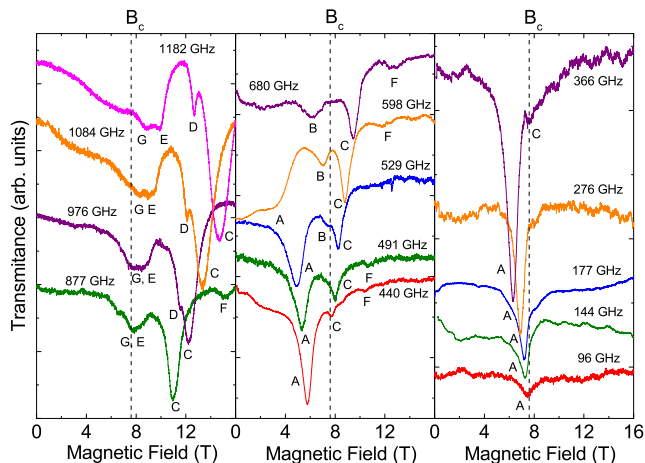


FIG. 3. Examples of unpolarized-ESR spectra in α -RuCl₃ for $H \parallel [100]$ at various frequencies; $T = 1.5$ K. The spectra are normalized by the zero-field transmittance background and offset for clarity. The vertical line indicates the critical field as determined in Ref. [9].

Several magnetic-resonance modes were observed above B_c . The frequency-field diagrams of these modes for different polarizations of the incident THz radiation are shown in Fig. 2.

Recent neutron-scattering measurements of α -RuCl₃ revealed a sharp magnon mode at the lower bound of a strong continuum [10]. This mode has a measurable dispersion in the direction perpendicular to the honeycomb planes, suggesting the presence of nonnegligible in-

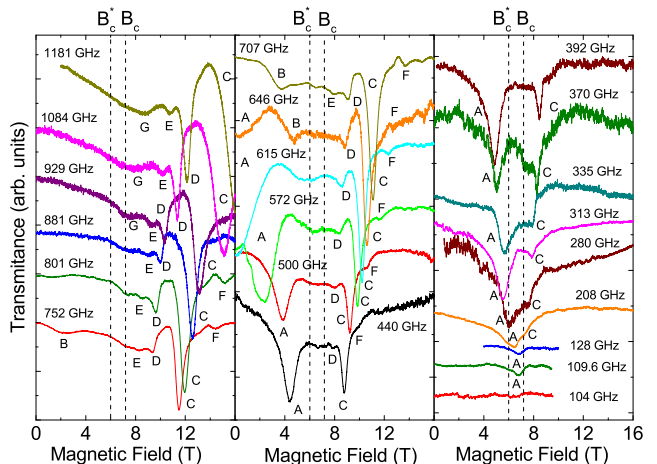


FIG. 4. Examples of unpolarized-ESR spectra in α -RuCl₃ for $H \parallel [110]$ and $T = 1.5$ K. The spectra are normalized by the zero-field transmittance background and offset for clarity. The vertical lines indicate critical fields as determined in Ref. [9].

terplane interactions (the dispersion perpendicular to the plane was seen also in the magnetically ordered phase below B_c , but it is much weaker than the in-plane dispersion). The corresponding neutron-scattering data at $(0,0,3.3)$ and $(0,0,4.3)$ are shown in Fig. 2(d) by closed squares and triangles, respectively. The dispersion periodicity along the $(0,0,L)$ direction suggests that the excitation energy at the Γ point (maximum of the excitation dispersion) and at the magnon zone boundary (dispersion minimum) are approximately the same as for $(0,0,3.3)$ and $(0,0,4.3)$, respectively. Based on that, the excitations C and F are identified as relativistic and exchange modes of magnetic resonance [Fig. 5(a)] [4]; similar excitations were observed, e.g., in the field-induced polarized phase in the triangular-lattice antiferromagnet Cs₂CuCl₄ [34]. The mode C is the most intensive resonance (Figs. 3 and 4), having maximal intensity for the polarization $h_\omega \perp H$. This mode was observed also by means of far-infrared [18, 20] and Raman-scattering [21] spectroscopy [the latter is denoted as M1 in Fig. 5(b)]. The mode F has a polarization $h_\omega \parallel H$. The corresponding transitions (modes C and F) are shown in Fig. 5(a) by the solid red and blue arrows, respectively. The observation of the exchange mode F (which is, as expected, much weaker than the mode C) becomes possible due to the staggered Dzyaloshinskii-Moriya interaction [35, 36], which is allowed in α -RuCl₃ due to the absence of an inversion symmetry center between the Ru ions in adjacent layers. Our scenario is supported by recent calculations for a three-dimensional exchange model [32]. The distance between the C and F modes gets larger with increasing field, indicating that spin correlations in the sys-

tem are becoming less 2D in high fields. Similar behavior was observed by inelastic neutron-scattering experiments [10].

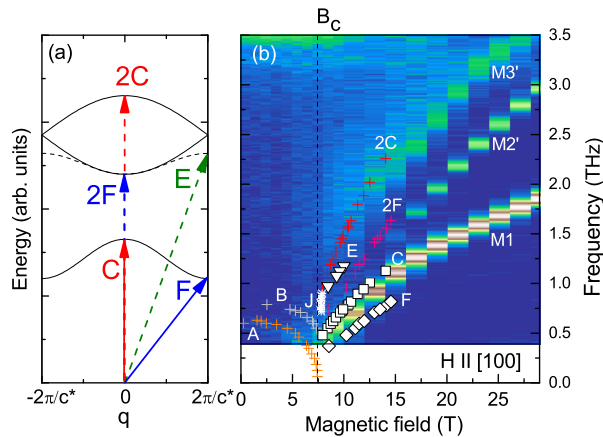


FIG. 5. (a) Proposed schematic energy diagram for α -RuCl₃ in an arbitrary magnetic field above B_c . The modes C and F are single-magnon excitations, while the modes 2C and 2F correspond to two-magnon excitations. The mode E corresponds to an excitation of a two-magnon bound state. (b) Frequency-field dependences of selected ESR modes [from Fig. 2(a) and Fig. 2(b)] and the color contour plot of the high-field Raman scattering intensity [21] ($H \parallel [100]$).

Raman scattering is known as a very powerful tool to probe two-particle processes in strongly correlated spin systems. Such two-magnon excitations, the modes M3' and M2', were observed in α -RuCl₃ in the field-induced phase [21, 37] (Fig. 5(b); for comparison we show simulated modes 2C and 2F with the excitation energy twice larger than that for the modes C and F, respectively). The continuum is spread well above 2C, suggesting contributions of multiple-particle processes in the entire Brillouin zone [32]. Based on the proposed scenario, one would expect the presence of higher-energy excitations (such as modes G and G* in Fig. 2), involving multiparticle processes with different wave numbers.

The ESR mode E, with excitation energy slightly larger than that for the mode 2F (but smaller than that for the mode 2C), was observed for $h_\omega \parallel H$ and can be tentatively interpreted as an excitation of a two-magnon bound state [dashed green arrow in Fig. 5(a)].

In the vicinity of B_c the modes G and E are superimposed (Fig. 3). To obtain more details about this critical range, we refer to our polarized-ESR measurement data (Supplemental Material [30]). Surprisingly, at about B_c our experiments revealed a broad dip, denoted as J, whose field position is almost independent on the frequency. The dip was observed in the $\sim 700 - 900$ GHz frequency range with the polarization of the incident THz radiation $h_\omega \parallel H$ ($H \parallel [100]$, Fig. 1(a), Supplemental Material) [38]. The position of the dip J is shown

in Figs. 2(a) and 5(b). Remarkably, these frequency range is located between modes 2F and 2C, corresponding to the lower and upper boundaries of the two-magnon continuum, respectively [Fig. 5]. This strongly suggests that the field-induced transition from the magnetically ordered to disordered phase strongly affects not only the ground state properties, but also the excitations spectrum, including multiparticles processes. We hope that our observation will stimulate further theoretical studies of the unconventional spin dynamics in α -RuCl₃, in particularly, in the critical regime in the vicinity of B_c .

The ESR mode D is relatively weak at low frequencies, gaining intensity at higher frequencies and fields. This mode is excited for both polarizations of incident THz radiation, $h_\omega \parallel H$ and $h_\omega \perp H$ (Fig. 2). Similar to other high-field modes, the resonance field for the mode D exhibits a 60° periodicity [15]. On the other hand, the angular dependence of this mode is significantly different from others (e.g., for modes C, E, F), demonstrating a shift of 30° . The observed very peculiar angular dependence of mode D might provide a potential hint for identifying the nature of this excitation.

Very recently, a plateau in the thermal-Hall-effect has been observed over a finite field range [39–41]. This has been interpreted as a signature of fractional non-Abelian excitations, possibly the Majorana fermions of the Kitaev model on a honeycomb lattice. The presence of a plateau over a limited range of applied fields (approximately between 9.7 and 11.5 T for $H \parallel [110]$ [40]) would suggest the presence of additional phase transitions at the fields corresponding to the upper and lower bounds of the plateau. Possible evidence for that has been seen in magnetocaloric [10] and magnetostriction [42] experiments, while another thermodynamic study (magnetic Grüneisen parameter and specific heat) detected no sign of such transitions [43]. Our high-field ESR measurements show magnon modes, characteristic of partially polarized state, emerging *right above* B_c , not revealing any evidence for additional high-field phases or phase transitions in magnetic fields up to 16 T. The question of such a coexistence (the nontrivial topological excitations, if any, and conventional bulk magnons, observed by us in α -RuCl₃) remains open, demanding more systematic experimental and theoretical investigations.

In conclusion, we have reported on the high-resolution high-field THz ESR spectroscopy studies of in-plane oriented single crystals of α -RuCl₃ in magnetic field up to B_c and beyond, applied parallel and perpendicular to Ru-Ru bond directions. We confirmed the rather anisotropic ESR response, highlighting significant role of anisotropic in-plane interactions in α -RuCl₃. Complemented by results of recent inelastic neutron- and Raman-scattering measurements, we argue that the high-field spin dynamics in this material is dominated by one- and two-particle excitations, identified as magnons.

This work was supported by the Deutsche Forschungs-

gemeinschaft (DFG), through ZV 6/2-2, the excellence cluster *ct.qmat* (EXC2147, project-id 390858490), and SFB 1143, as well as by the HLD at HZDR, member of the European Magnetic Field Laboratory (EMFL). A. Banerjee and S. E. Nagler were supported by the Division of Scientific User Facilities, Basic Energy Sciences US DOE, P. Lampen-Kelley and D. G. Mandrus by the Gordon and Betty Moore Foundation's EPIQS Initiative through Grant GBMF4416, J.-Q. Yan and C. A. Bridges by the U.S. Department of Energy, Office of Science, Office of Basic Energy Sciences, Materials Sciences and Engineering Division. We would like to thank D. Wulferding and P. Lemmens for sharing their experimental data. We acknowledge discussions with M. Vojta, A. Chernyshev, M. Zhitomirsky, and A. Kolezhuk.

Supplemental Material

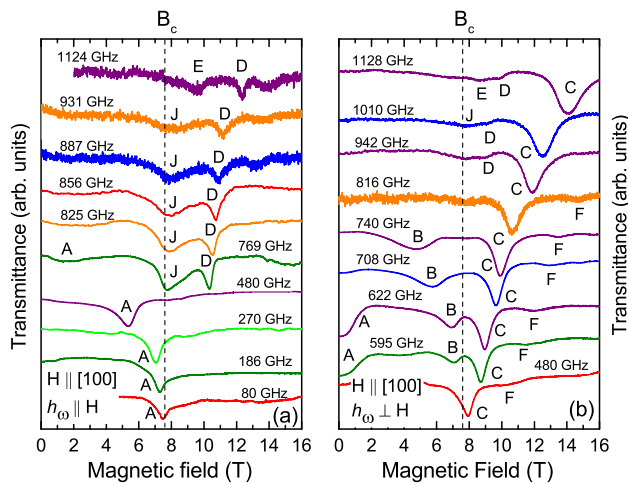


FIG. 6. Examples of polarized-ESR spectra in α -RuCl₃ for $h_\omega \parallel H$ (a) and $h_\omega \perp H$ (b) (h_ω is the magnetic component of the THz radiation). $H \parallel [100]$, $T = 1.5$ K. The spectra are normalized by the zero-field transmittance background and offset for clarity. The vertical line indicates the critical field as determined in Ref. [9].

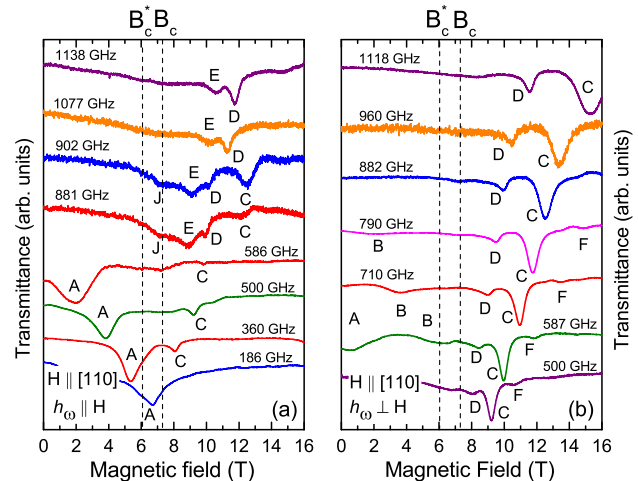


FIG. 7. Examples of polarized-ESR spectra in α -RuCl₃ for $h_\omega \parallel H$ (a) and $h_\omega \perp H$ (b) (h_ω is the magnetic component of the THz radiation). $H \parallel [110]$, $T = 1.5$ K. The spectra are normalized by the zero-field transmittance background and offset for clarity. The vertical lines indicate the critical fields as determined in Ref. [9].

* Present Address: Institute of Radiation Physics, Helmholtz-Zentrum Dresden-Rossendorf, 01328 Dresden, Germany

† Present Address: Department of Physics and Astronomy, Purdue University, West Lafayette, IN 47907, U.S.A.

‡ s.zvyagin@hzdr.de

[1] J. Chaloupka, G. Jackeli, and G. Khaliullin, Phys. Rev. Lett. **105**, 027204 (2010).
[2] A. Kitaev, Ann. Phys. **321**, 2 (2006).

[3] K. W. Plumb, J. P. Clancy, L. J. Sandilands, V. V. Shankar, Y. F. Hu, K. S. Burch, H. Y. Kee, and Y. J. Kim, Phys. Rev. B **90**, 041112(R) (2014).
[4] P. A. Maksimov and A. L. Chernyshev, arXiv:2004.10753.
[5] J. A. Sears, M. Songvilay, K. W. Plumb, J. P. Clancy, Y. Qiu, Y. Zhao, D. Parshall, and Y.-J. Kim, Phys. Rev. B **91**, 144420 (2015).
[6] R. D. Johnson, S. C. Williams, A. A. Haghighirad, J. Singleton, V. Zapf, P. Manuel, I. I. Mazin, Y. Li, H. O. Jeschke, R. Valentí, and R. Coldea, Phys. Rev. B **92**, 235119 (2015).
[7] Due to the presence of the finite Kitaev coupling, a full spin polarization can be achieved only at infinitely large magnetic field.
[8] A. Banerjee, P. Lampen-Kelley, J. Knolle, Ch. Balz, A. A. Aczel, B. Winn, Y. Liu, D. Pajerowski, J. Yan, C. A. Bridges, A. T. Savici, B. C. Chakoumakos, M. D. Lumsden, D. A. Tennant, R. Moessner, D. G. Mandrus, and S. E. Nagler, npj Quantum Materials **3**, 8 (2018).
[9] P. Lampen-Kelley, L. Janssen, E. C. Andrade, S. Rachel, J.-Q. Yan, C. Balz, D. G. Mandrus, S. E. Nagler, and M. Vojta, arXiv:1807.06192.
[10] C. Balz, P. Lampen-Kelley, A. Banerjee, J. Yan, Z. Lu, X. Hu, S. M. Yadav, Y. Takano, Y. Liu, D. A. Tennant, M. D. Lumsden, D. Mandrus, and S. E. Nagler, Phys. Rev. B **100**, 060405(R) (2019).
[11] L. J. Sandilands, Y. Tian, K. W. Plumb, Y. J. Kim, and K. S. Burch, Phys. Rev. Lett. **114**, 147201 (2015).
[12] A. Banerjee, J. Yan, J. Knolle, C. A. Bridges, M. B. Stone, M. D. Lumsden, D. G. Mandrus, D. A. Tennant, R. Moessner, and S. E. Nagler, Science **356**, 1055 (2017).
[13] S.-H. Do, S.-Y. Park, J. Yoshitake, J. Nasu, Y. Motome,

- Y.-S. Kwon, D. T. Adroja, D. J. Voneshen, K. Kim, T.-H. Jang, J.-H. Park, K.-Y. Choi, and S. Ji, *Nat. Phys.* **13**, 1079 (2017).
- [14] A. Banerjee, C. A. Bridges, J.-Q. Yan, A. A. Aczel, L. Li, M. B. Stone, G. E. Granroth, M. D. Lumsden, Y. Yiu, J. Knolle, D. L. Kovrizhin, S. Bhattacharjee, R. Moessner, D. A. Tennant, D. G. Mandrus, and S. E. Nagler, *Nat. Mat.* **15**, 733 (2016).
- [15] A. N. Ponomaryov, E. Schulze, J. Wosnitza, P. Lampen-Kelley, A. Banerjee, J.-Q. Yan, C. A. Bridges, D. G. Mandrus, S. E. Nagler, A. K. Kolezhuk, and S. A. Zvyagin, *Phys. Rev. B* **96**, 241107(R) (2017).
- [16] A. Little, L. Wu, Liang, P. Lampen-Kelley, A. Banerjee, S. Patankar, D. Rees, C. A. Bridges, J. Q. Yan, D. Mandrus, S. E. Nagler, and J. Orenstein, *Phys. Rev. Lett.* **119**, 227201 (2017).
- [17] L. Wu, A. Little, E. E. Aldape, D. Rees, E. Thewalt, P. Lampen-Kelley, A. Banerjee, C. A. Bridges, J.-Q. Yan, D. Boone, S. Patankar, D. Goldhaber-Gordon, D. Mandrus, S. E. Nagler, E. Altman, and J. Orenstein, *Phys. Rev. B* **98**, 094425(R) (2018).
- [18] Z. Wang, S. Reschke, D. Huvonen, S.-H. Do, K.-Y. Choi, M. Gensch, U. Nagel, T. Rom, and A. Loidl, *Phys. Rev. Lett.* **119**, 227202 (2017).
- [19] C. Wellm, J. Zeisner, A. Alfonsov, A. U. B. Wolter, M. Roslova, A. Isaeva, T. Doert, M. Vojta, B. Buchner, and V. Kataev, *Phys. Rev. B* **98**, 184408 (2018).
- [20] A. Sahasrabudhe, D. A. S. Kaib, S. Reschke, R. German, T. C. Koethe, J. Buhot, D. Kamenskyi, C. Hickey, P. Becker, V. Tsurkan, A. Loidl, S. H. Do, K. Y. Choi, M. Gruninger, S. M. Winter, Z. Wang, R. Valentı, and P. H. M. van Loosdrecht, *Phys. Rev. B* **101**, 140410(R) (2020).
- [21] D. Wulferding, Y. Choi, S.-H. Do, C.-H. Lee, P. Lemmens, C. Faugeras, Y. Gallais, and K.-Y. Choi, *Nat. Commun.* **30** 1603 (2020).
- [22] S. M. Winter, K. Riedl, P. A. Maksimov, A. L. Chernyshev, A. Honecker, and R. Valentı, *Nat. Commun.* **8**, 1152 (2017).
- [23] S. M. Winter, K. Riedl, D. Kaib, R. Coldea, and R. Valentı, *Phys. Rev. Lett.* **120**, 077203 (2018).
- [24] P. Lampen-Kelley, S. Rachel, J. Reuther, J.-Q. Yan, A. Banerjee, C. A. Bridges, H. B. Cao, S. E. Nagler, and D. Mandrus, *Phys. Rev. B* **98**, 100403(R) (2018).
- [25] T. Suzuki and S. Suga, *AIP Adv.* **8**, 101414 (2018).
- [26] T. Asano, H. Nojiri, Y. Inagaki, J. P. Boucher, T. Sakon, Y. Ajiro, and M. Motokawa, *Phys. Rev. Lett.* **84**, 5880 (2000).
- [27] S. A. Zvyagin, A. K. Kolezhuk, J. Krzystek, and R. Feyerherm, *Phys. Rev. Lett.* **93**, 027201 (2004).
- [28] K. Yu. Povarov, A. I. Smirnov, O. A. Starykh, S. V. Petrov, and A. Ya. Shapiro, *Phys. Rev. Lett.* **107**, 037204 (2011).
- [29] A. A. Validov, M. Ozerov, J. Wosnitza, S. A. Zvyagin, M. M. Turnbull, C. P. Landee, G. B. Teitelbaum, *J.Phys.-Cond. Matt.* **26**, 026003 (2014).
- [30] Supplemental Material.
- [31] S. A. Zvyagin, J. Krzystek, P. H. M. van Loosdrecht, G. Dhahenne, and A. Revcolevschi, *Physica B* **346-347**, 1 (2004).
- [32] L. Janssen, S. Koch, and M. Vojta, *Phys. Rev. B* **101**, 174444 (2020).
- [33] C. Balz et al., unpublished.
- [34] S. A. Zvyagin, D. Kamenskyi, M. Ozerov, J. Wosnitza, M. Ikeda, T. Fujita, M. Hagiwara, A. I. Smirnov, T. A. Soldatov, A. Ya. Shapiro, J. Krzystek, R. Hu, H. Ryu, C. Petrovic, and M. E. Zhitomirsky, *Phys. Rev. Lett.* **112**, 077206 (2014).
- [35] V. G. Bar'yakhtar, V. V. Yeremenko, V. M. Naumenko, Y. G. Pashkevich, V. V. Pishko, and V. L. Sobolev, *Sov. Phys. JETP* **61**, 823 (1985).
- [36] T. Sakai and H. Shiba, *J. Phys. Soc. Jpn.* **63**, 867 (1994).
- [37] Contrary to our interpretation, the mode $M2'$ in Ref. [21] is identified as excitation of a two-magnon bound state.
- [38] The dip J is more pronounced for $H \parallel [100]$, but some signature of this feature was observed for $H \parallel [110]$ (see, e.g., the spectrum at 881 and 902 GHz in Fig. 2(a), Supplemental Material).
- [39] Y. Kasahara, T. Ohnishi, N. Kurita, H. Tanaka, J. Nasu, Y. Motome, T. Shibauchi, and Y. Matsuda, *Nature* **559**, 227 (2018).
- [40] T. Yokoi, S. Ma, Y. Kasahara, S. Kasahara, T. Shibauchi, N. Kurita, H. Tanaka, J. Nasu, Y. Motome, C. Hickey, S. Trebst, and Y. Matsuda, arXiv:2001.01899.
- [41] M. Yamashita, N. Kurita, and H. Tanaka, arXiv:2005.00798.
- [42] S. Gass, P. M. Consoli, V. Kocsis, L. T. Corredor, P. Lampen-Kelley, D. G. Mandrus, S. E. Nagler, L. Janssen, M. Vojta, B. Buchner, and A. U. B. Wolter, arXiv:2003.07081.
- [43] S. Bachus, D. A. S. Kaib, Y. Tokiwa, A. Jesche, V. Tsurkan, A. Loidl, S. M. Winter, A. A. Tsirlin, R. Valentı, and P. Gegenwart, arXiv:2006.02428.